Classification of Live / Lifeless Assets from Long Distance with Laser Signals by Using Deep Learning Network

Nevzat Olgun^{1*}, İbrahim Türkoğlu²

¹ Zonguldak Bulent Ecevit University, Department of Computer Technologies, 67800, Devrek/Zonguldak, Türkiye.

²Firat University, Department of Software Engineering, 23200, Merkez/Elazığ, Türkiye.

*Corresponding Author email: nevzat.olgun@beun.edu.tr

Abstract

In counter-terrorism, urban warfare operations and active combat environments, some targets may be live people, while some targets may consist of fake materials such as mannequins. Determining whether these targets are alive or not is important for human life. In addition, it is important to determine whether the instruments used in the biometric verification steps belong to a real living thing. In this study, it is aimed to classify the determined targets as live/lifeless with low-power laser signals in situations where people cannot be reached directly. For this purpose, people as living samples and different types of lifeless materials at a certain distance were pointed with a low-powered laser light source and laser signals reflected from the targets were recorded with the receiving system. In the classification of Live / Lifeless, human vitality and other materials (non-living) in nature are compared. In the study, laser signal samples are taken from different points of the arm of 9 volunteer men for living assets and 17 materials frequently used by people for lifeless assets. For lifeless assets, often found in nature, aluminum, black, fabric, frosted glass, glass, pottery, iron, galvanize, granite, linden, magnet, mdf, marble, cardboard, polyethylene, polystyrene, PVC and artificial marble are selected. The laser signals obtained from the targets are classified as live/lifeless by undergoing training in Long-Short Term Memory networks after preprocessing and feature extraction steps. As a result of the study, a live / lifeless assets distinction is made with an accuracy rate of 99.7%.

Key words

Laser, Laser Signs, Deep Learning, Liveness Detection, Live Detection, Target Detection

1. INTRODUCTION

It is important to determine the vitality of the elements on the enemy front line in active war environments, in the fight against terrorism and in urban warfare operations. In some cases, mannequin and similar materials are used in the elements on the enemy line and if this can be detected remotely, significant gains can be achieved. In such cases, it is important to determine the presence of live / inanimate assets of the target from far distances with laser signals. Similarly, if real live targets can be detected in hostage operations, many lives can be saved.

In addition, in biometric security systems, it is important to detect vitality in order to determine whether the fingerprint, photograph, retina belong to a living person. In this way, interference that imitates a person's biometric

data can be detected and necessary precautions can be taken. Printed photographs of the human face, patterns for fingerprints, and 3D masks for face detection are frequently used to overcome biometric measures [1–3].

Many studies have been carried out on viability detection in the literature. Some of these studies focused on radio frequency, some on cameras, and some on lasers. In the literature, there are studies on the localization of a person behind the wall with the wall radar and signs of life [4–7]. The focus of such studies is to take advantage of the micro-doppler characteristic caused by small vibrations in the body during human breathing. In such systems, a radio frequency signal is sent to the body, and when the signal reaches the body, small displacement information is returned as a phase shift signal due to breathing or heartbeat movement.

In vitality detection studies with a camera, methods such as obtaining heart rate information, detecting blinking movements, detecting facial mimics, color gradient features are frequently used [1–3,8–20]. In vitality detection applications where camera systems are used, the system fails in insufficient light conditions or in cases where there is no light at all.

One of the techniques used in vitality detection that allows for non-contact measurement is the use of lasers. Lasers have also become an important tool for optical remote sensing due to their ability to produce an intense amount of parallel beam consisting of monochromatic, coherent and polarized light. For the first time, there have been great developments in the production techniques of lasers produced using ruby crystal over time, and varieties operating at different wavelengths, different output powers and different pulse times have emerged [21]. According to the material used in the production of lasers, they are divided into four groups as gas lasers, liquid lasers, solid state lasers and semiconductor (diode) lasers. While lasers used in continuous wave form transmit a relatively low amount of energy to the target continuously, lasers in pulsed wave form can transmit instantaneously higher energy to the target at certain intervals. Diode lasers are small in size and low cost, they can be produced at different output powers and different wavelengths. Because of these advantages, they are frequently used in chemical analysis, remote sensing, medical applications, defense technologies, telecommunications and industry [22].

When laser light is reflected on a target object, it is partially reflected, partially transmitted, or partially absorbed from the target. Laser beams reflected from the target can be measured and converted into signals with the help of high gain coefficient avalanche photo diodes in electro-optic devices. Due to the fact that different types of targets exhibit scattering and absorption properties in different ways, it is possible to obtain information about many types of living/lifeless targets around us using laser signals reflected from targets.

Very small amounts of mechanical vibrations can be measured with laser interferometers [23–27]. With traditional Michelson interferometer-based laser vibration meters, it can measure heartbeats and skin changes during breathing at close range [28–30]. Such interferometers require stable optical setup and are not suitable for use outside the laboratory. Laser Doppler Vibrometers (LDV) are laser vibration meters that are widely used in measuring small vibrations and are also commercially available on the market [31]. In a study with LDV, vibrations in the chest wall as a result of beating of the heart were measured and the results were associated with ECG [32]. In another study, the vibrations of the skin surface in the neck are studied depending on the cardiac rate[33,34]. Qu et al. have worked on the detection of human voice using pan-tilt-zoom (PTZ) camera and LDV. In this study, they focused on the detection of the moving person with the PTZ camera and the orientation of the LDV on the moving person for sound detection with LDV [35].

Marchionni et al. used LDV to measure heart and lung activities from a distance of about 2 m in preterm children[36]. Takano et al., in their study, reflected a laser beam on the subjects' face and recorded the laser spots formed for 30 seconds with a time-lapse camera. They extracted the subjects' heart rate information from the video recordings [37]. Ozana et al., in their study on farm animals, projected a laser light source to the targets and recorded the laser spots on the target with a 500-fps camera. They obtained the heart rate and respiratory information of the subjects with the signal processing methods from the video they recorded [38].

In the previous studies carried out by our team, a single laser light source and receiver system are used to classify different types of lifeless materials at a distance [39,40].

In this study, when health teams such as earthquakes, floods, storms, war environments and falls from height cannot reach the patient directly, or when it is necessary to determine the viability of elements on the enemy front line in a combat environment, it is necessary to collect information with low power laser signs from the specified target and in the light of the information obtained, it is intended to be classified as life/lifeless. In the classification of live/lifeless, human vitality and other materials (non-living) in nature are compared. Within the scope of the study, laser signals are obtained from a certain distance from live and lifeless targets, the obtained signals are classified as live/lifeless by undergoing training in Long-Short Term Memory networks (LSTM) after preprocessing and feature extraction steps and the results are examined.

When the literature is examined, it is seen that cameras are generally used in livelihood detection studies. Ambient light plays an important role in systems where cameras are used. In low lighting conditions, the performance of

the systems made with the camera decreases. In cases where there is insufficient or no ambient light, camera systems become completely inoperable. With the proposed system, an active measurement method using only laser light is presented. This study with laser light has the potential to be less affected by lighting conditions. The main contributions of this study are as follows.

- Live/lifeless classification was made using a laser signal and deep learning architecture based on a single measurement point.
- A faster classification time was obtained by using reduced size laser signals instead of raw laser signals in the detection of live/lifeless.
- Classification of different types of lifeless assets and a living human tissue was performed based on laser signals and deep learning.

2. RELATED WORKS

In this section, general information about the basics of laser measurement technique, which is the basis of the distinction between living tissue and lifeless materials, and the deep learning model used in classification are given.

2.1. Interaction of laser light with materials and living tissue

When laser beams are reflected on the surface of a material, they make specular or diffuse reflections depending on the surface roughness of the material. When the amount of roughness on the surface of the material is smaller than the wavelength of the laser light reflected on the material, specular reflection will occur, otherwise diffuse reflection will occur [40]. In cases where there is diffuse reflection, subsurface scattering occurs. Under natural conditions, many materials have a certain amount of rough surface due to the micro-textures on their surface. In this case, the laser beams reflected on the material reflect as a combination of specular and diffuse reflection. Figure 1 shows specular and diffuse reflection patterns of laser beams from the material surface. As can be seen in Figure 1, subsurface scattering can also occur in diffuse reflections. Since each material type has different surface textures and different microstructures, the laser signals reflected from the materials will also be different.

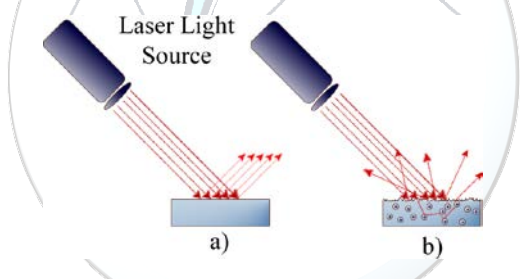


Figure 1. Laser beams and reflection types a) Specular reflection from a smooth surface b) Diffuse reflection and subsurface scattering from a rough surface

Lasers are in different wavelengths according to the production technique. Laser beams of different wavelengths and different optical output power can cause different effects on living tissues. When laser beams are projected onto a tissue, they show reflection, absorption, transmission and scattering [41]. Depending on the wavelength, the interaction of laser beams with living tissue can also be a mixture of them. Figure 2 shows the interaction of laser beams with living tissue. In this study, laser signals reflected from living tissue were used. The reflection amount of laser beams between 300-1100nm wavelength in soft tissues is 10 times higher than absorption.

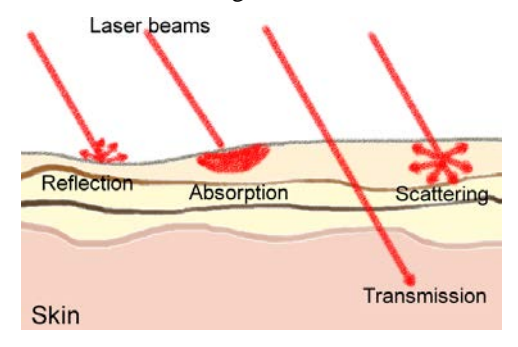


Figure 2. Interaction of laser beams with living tissue. Depending on the characteristics of the laser and the living tissue, the laser beam reflects, absorbs, transmits or scatters.

2.2. Deep learning: LSTM model

The use of Deep learning algorithms has started to increase in many areas such as object recognition, signal processing, natural language processing. Deep learning is a type of artificial neural networks (ANN). The most important step in artificial neural networks and other machine learning algorithms is extracting properties from raw data [42]. This step is no longer required with use of deep learning networks. Deep learning networks can extract features from the raw data given to them due to their structure and transfer this important data as an input to the next layer [43].

Deep learning networks consist of different architectures according to the areas in which they are used. Convolutional neural networks (CNN) are often used in image processing and similar fields [42,44]. In addition, CNNs are used in signal processing [45,46]. Recurrent neural networks (RNN) architecture is frequently used in signal processing, natural language processing, and time series data processing [47–50]. RNN focuses on the relationship between the data in the input sequence given to it. Cells in this architecture use their outputs as input in the next process. In this case, the output of each cell depends on the previous output. A simple RNN cell and its expansion can be seen in Figure 3.

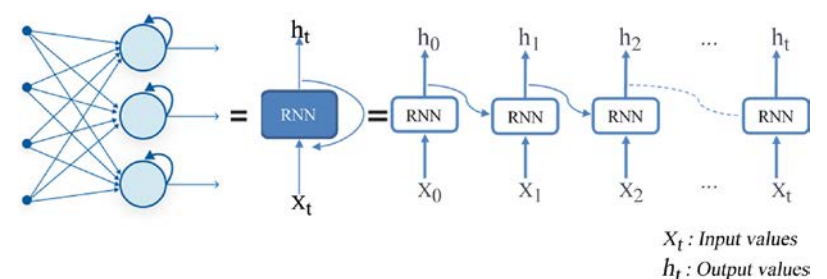


Figure 3. RNN cell and its expansion

RNN architecture succeeds in short-term dependencies but fails in long-term dependencies. Hochreiter et al. reported that the problem related to learning of long-term dependencies in RNN architecture was solved in their study made in 1997. This structure similar to RNN is called Long Short-Term Memory networks (LSTM). LSTM consists of a memory cell that can protect its state over time and non-linear gates regulating data input/output in the cell [40,51]. Input, forget, and output gates in an LSTM cell is interconnected by 4 neural networks and they form the cell memory. LSTM model, gates in its structure as well as the internal structure of an LSTM cell can be seen in Figure 4.

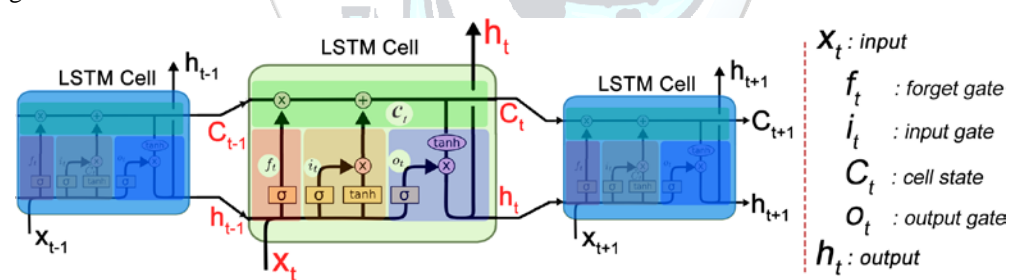


Figure 4. LSTM model, gates in its structure and the internal structure of the LSTM cell

In LSTM cell model shown in Figure 4, out of the forget gate is represented by f_t , out of the input gate by i_t whereas out of the output gate is represented by o_t , the cell state by C_t and out of the cell by h_t . f_t , i_t , C_t , o_t and h_t are defined in Eq. 1 - 5. Weights are represented by W_f , W_i , W_c , W_o , bias values are represented by b_f , b_i , b_c , b_o [40].

$$f_t = \sigma(W_f \cdot [h_{t-1}, x_t] + b_f) \tag{1}$$

$$i_t = \sigma(W_i \cdot [h_{t-1}, x_t] + b_i) \tag{2}$$

$$C_t = f_t * C_{t-1} + i_t * [tanh(W_c \cdot [h_{t-1}, x_t] + b_c)]$$
(3)

$$o_t = \sigma(W_0 \cdot [h_{t-1}, x_t] + b_0) \tag{4}$$

$$h_t = o_t * tanh(C_t) \tag{5}$$

3. MATERIALS AND METHODS

3.1. Experimental Setup and Data Collection

Laser meter module that emits red light at 1 mW output power and 650 nm wavelength is used in the scope of the study. The firmware of the laser meter module is reprogrammed to take 3000 raw laser mark samples per measurement and transfer them to the computer via the serial port [39]. Different points of the live / lifeless targets in the laboratory environment are pointed with the laser light source on the cartesian robot arm in line with the coordinates coming from the computer program, and the laser signals reflected from the target are detected by the device and transferred to the computer system. The distance between the laser light source and the targets is chosen as 2 meters. In Figure 5, the sensor module consisting of the experimental study setup, laser light source and optical device are shown.

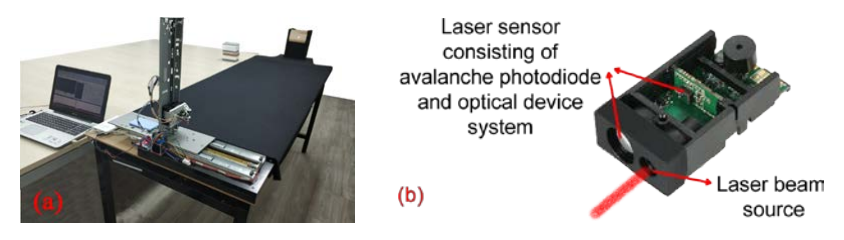


Figure 5. a) Experimental work setup.

b) Laser light source and optical system.

In the study conducted during daylight hours, 130 laser signal samples are taken from different points of the arm of 9 volunteer men for live assets, and 69 laser signal samples from different points of 17 materials frequently used by people for lifeless assets. Aluminum, black fabric, frosted glass, glass, pottery, iron, galvanize, granite, linden, magnet, mdf, marble, cardboard, polyethylene, polystyrene, pvc and artificial marble are selected for lifeless assets. In Figure 6, the visuals of the materials used in the study and the position of living and inanimate beings in the experimental setup are shown. In addition, before each measurement, measurements are made by turning off the laser light to detect white noise caused by the device and daylight. At the end of the data collection process, a total of 1170 laser signals are obtained from the arms of male subjects and a total of 1170 laser signals from lifeless assets.

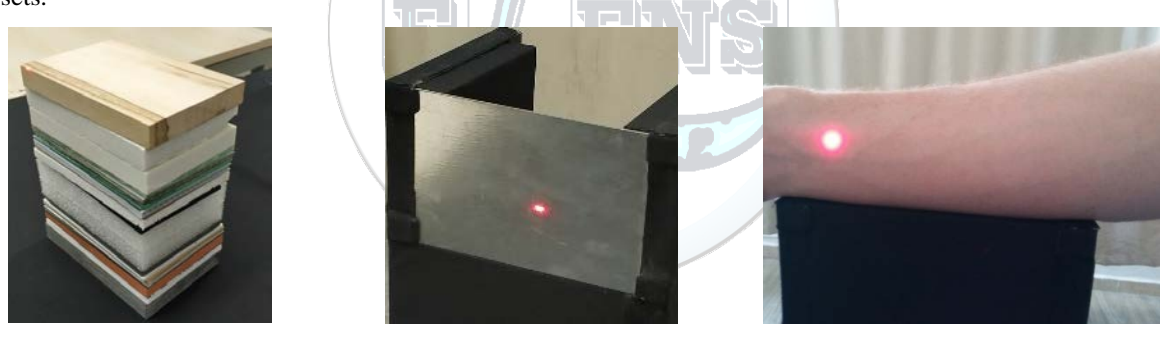


Figure 6. Images of the materials used in the study and the position of live/lifeless assets in the experimental system.

3.2. Signal Processing and Deep Learning

The study consists of steps for data collection, data preparation and classification. Figure 7 shows the block diagram of the study.

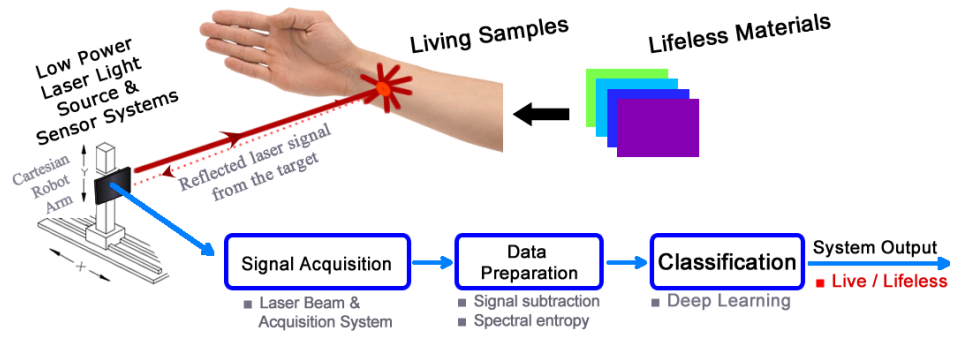


Figure 7. Block diagram of the study

In the preprocessing step of the study, the subtraction process defined in Equation 6 is performed to separate the environment & system noise signals from the laser signals obtained from live and lifeless assets.

$$x(n) = s(n) - d(n) \tag{6}$$

In Equation 6, x(n) refers to the noise-free laser signal, s(n) refers to the noisy laser signal, and d(n) refers to the environment & system noise signals. In Figure 8, the raw laser signals of the male subject's arm, aluminum, linden(wood) and pottery are seen, environment & system noise signals are seen and the laser signals as a result of the subtraction process are seen.

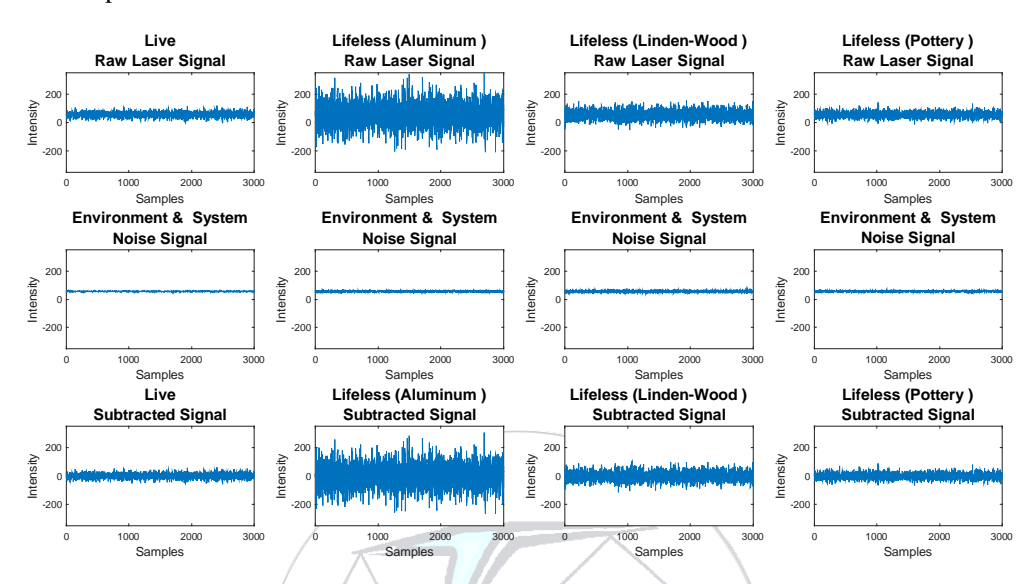


Figure 8. Raw laser signals of live, lifeless(aluminum), lifeless(linden), lifeless(pottery) materials, environment & system noise signals and the laser signals as a result of the subtraction process

The normalized energy distribution graph of the raw laser signals obtained after subtracting the background noise signals from the raw signals obtained from living and lifeless assets is given in Figure 9.

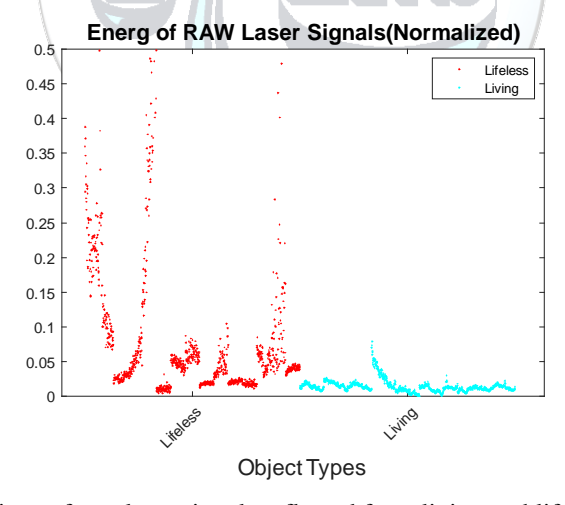


Figure 9. Energy distributions of raw laser signals reflected from living and lifeless assets after subtraction process

The spectral power density is based on the process of estimating the power distribution in the frequency band of the signal. This process is based on the Fourier transform. Welch method is an advanced version of this method [31]. The Welch spectral power density is explained as in Equation 7.

$$P_{w} = \frac{1}{l} \sum_{i=0}^{l-1} \check{S}_{xx}^{i}(f) \tag{7}$$

In Equation 7, P_w shows Welch spectral power density, $S_{xx}^i(f)$ shows the i^{th} improved periodogram of spectral power density, and l shows the length of the signal. In the study, Welch spectral power density is applied to laser signals following subtraction process. Figure 10 shows the laser signals with subtraction process and laser signals with Welch spectral power density applied.

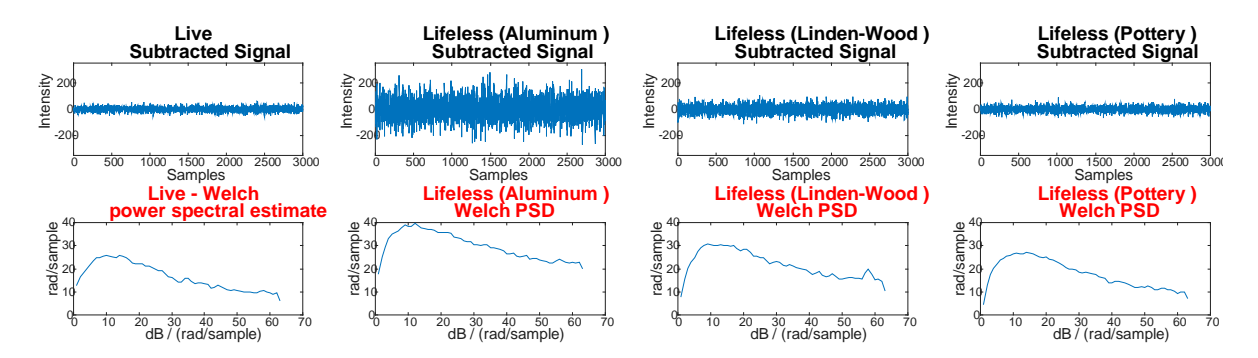


Figure 10. Preprocessed laser signals for live, lifeless(aluminum), lifeless (galvanize) materials and laser signals with Welch spectral power density applied

In the study, a bidirectional LSTM architecture consisting of 64 hidden layers are used to classify laser signals from a total of 2340 live/lifeless assets obtained as a result of signal processing steps. Figure 11 shows the LSTM architecture used in the study. In the study, the number of hidden layers, layer structures and hidden unit numbers in the layers were selected by trial-and-error method.

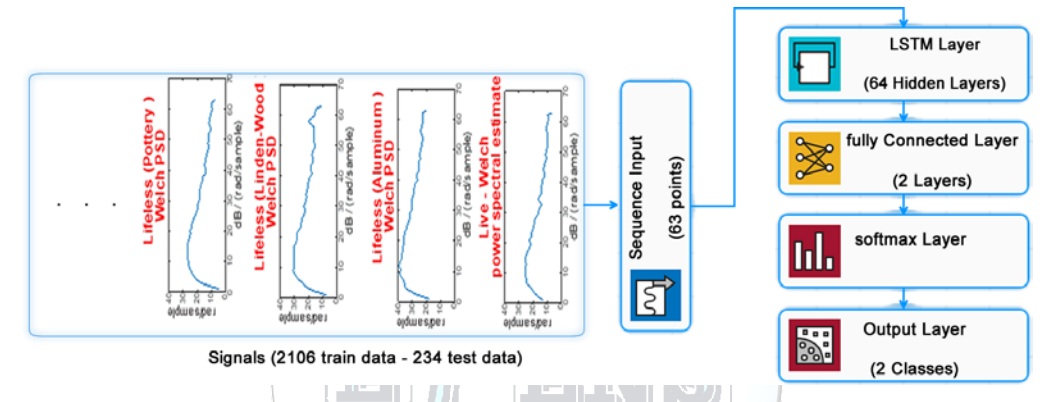


Figure 11. LSTM architecture used in the study

3.3. Performance Evaluation

In this study, the performance of the proposed model was evaluated using a 10-fold cross validation technique. This technique avoids obtaining biased results in validation results [52]. The data set obtained was randomly divided into 10 equal parts so that the amount of data in each class was equal. While 9 parts of the data set divided into parts were used for training the model, the remaining part was used for the performance test of the model. This process was done for all parts of the data set and the overall performance of the system was found by averaging the results obtained from the test results. The graphical model of training and test data according to the 10-fold cross-validation technique can be seen in Figure 11.

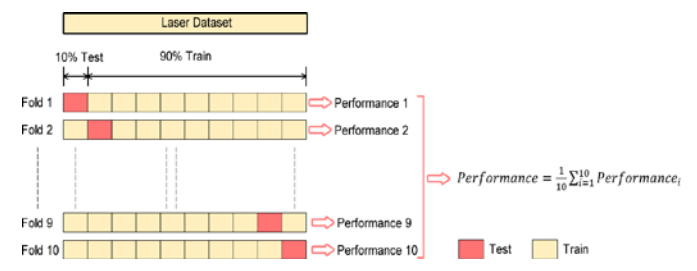


Figure 11. Graphical model of training and test data according to 10-fold cross validation technique.

Classification accuracy was used to compare the proposed system with existing studies. It is extremely important to use the same performance criteria to make comparative assessments with existing studies. Most of the existing studies use accuracy criteria in classification. Considering the accuracy criterion is a reasonable criterion in studies where the data set is balanced. The accuracy criterion can be defined as the ratio of the estimates that the classifier makes correctly to all estimates. The accuracy of the proposed method can be calculated as in Eq. 8.

$$Accuracy = \frac{TP + TN}{TP + TN + FP + FN} \tag{8}$$

True positive (TP), true negative (TN), false positive (FP), and false negative (FN) were taken as basis for the calculation of accuracy performance criteria. In this study, precision, recall and F-score evaluation criteria were used as well as accuracy performance criteria. These definitions are shown in the following equations [53].

$$precision = \frac{TP}{TP + FP} \tag{9}$$

$$recall = \frac{TP}{TP + FN} \tag{10}$$

$$F - score = 2 * \frac{precision * recall}{precision + recall}$$
(11)

4. RESULTS AND DISCUSSION

In LSTM architecture, which is used for classification of live and lifeless assets, the data set is divided into 10 equal parts, and the remaining data is used for training at a time. The hyper parameters used for the training of the LSTM network were determined as the maximum epoch number of 100, the learning rate 0.001, and the optimization algorithm Adam. Mini-batch size was chosen as 256.

The length of the raw laser signals obtained from the experimental studies consists of 3000 points. Measurements were taken with the laser beams on and off to eliminate environment/device noise. During the data preparation phase, these signals were subtracted from each other and the noise in the signals was removed. As it is known, processing high-dimensional signals in deep learning models is time consuming and costly. For this reason, the noise-free raw laser signals were converted into signals of much smaller size (63 points) by calculating the Welch spectral power densities. In the experimental studies, the reduced size laser signals were trained separately in 16, 32, 64, 128 hidden layer LSTM networks and their performances were compared. The calculation time of a signal from the raw laser signal according to the Welch method took 0.026 s.

Training of reduced size laser signals in the LSTM model significantly increases the performance and speed of the system. With the reduction of the data size, the training time in the 64 hidden layer LSTM network takes 0.55 seconds per epoch. Average classification results, training times and LSTM hidden layer numbers of the reduced size laser signals are given in Table 1.

Table 1. Hidden layers, average classification results and training times of laser signals with reduced dimensions.

LSTM Hidden Layer	16	32	64	128
Training time (1 epoch)	0.39 s	0.44 s	0.55 s	0.87 s
Recall	% 97.42 ± 4.38	99.29 ± 0.81	$\%$ 99.70 \pm 0.45	$\%$ 99.49 \pm 0.44
Precision	$\%97,39 \pm 4,42$	$\%99.27 \pm 0.83$	$\%99.70 \pm 0.45$	$\%99.49 \pm 0.44$
F1-score	% 97,41± 4,40	$\%$ 99.28 \pm 0.82	$\%$ 99.70 \pm 0.45	$\%$ 99.49 \pm 0.44
Accuracy	% 97.39 ± 4.42	% 99.27 ± 0.83	% 99.70 ± 0.45	% 99.49 ± 0.44

After the training of the network, the classification performance in the test data is calculated as the lowest 98.72%, the highest 100% and the average performance is 99.70%. Figure 12 shows the confusion matrix of the highest training and test performance of the 64 hidden layers LSTM network.

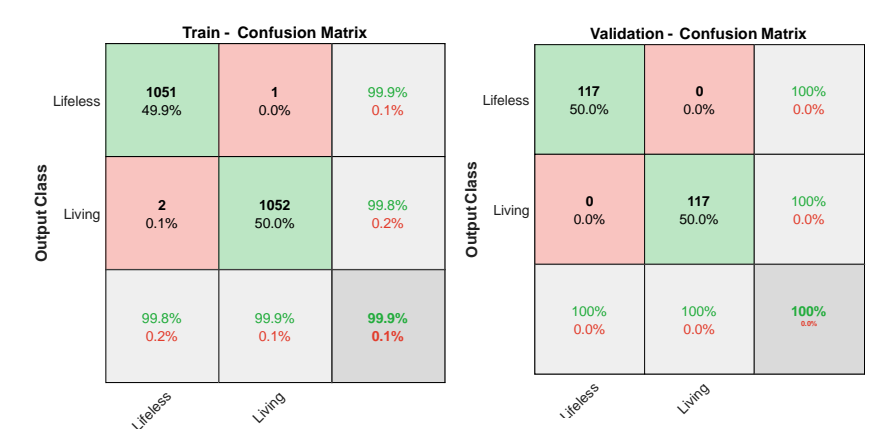


Figure 12. Confusion matrix showing the highest results in the classification performance of live and lifeless assets.

In this study, it is aimed to classify the target determined by low-power laser signals from a certain distance as live/lifeless when it is necessary to detect the vitality of the elements on the enemy front line in the war environment or to determine whether the people using biometric verification systems are real people. For this purpose, laser signals are obtained from the arms of the volunteer subjects and 17 materials, the laser signals obtained are passed through the signal processing steps and they are trained and classified using the LSTM architecture used in deep learning networks. With the proposed system, a high performance of 99.70% has been achieved.

In later studies, the classification of the target from more distances and the effect of atmospheric conditions on the performance of the system can be examined.

REFERENCES

- [1] Singh M, Arora AS. A Novel Face Liveness Detection Algorithm with Multiple Liveness Indicators. Wireless Personal Communications 2018;100:1677–87. https://doi.org/10.1007/S11277-018-5661-1.
- [2] Matthew P, Anderson M. Novel categorisation techniques for liveness detection. Proceedings 2014 8th International Conference on Next Generation Mobile Applications, Services and Technologies, NGMAST 2014 2014:153–8. https://doi.org/10.1109/NGMAST.2014.51.
- [3] Fei J, Xia Z, Yu P, Xiao F. Adversarial attacks on fingerprint liveness detection. Eurasip Journal on Image and Video Processing 2020;2020:1–11. https://doi.org/10.1186/S13640-020-0490-Z/TABLES/7.
- [4] Debnath SBC. TTW life sign detection by means of CW X-band radar, homeland security and rescue applications. 2017 USNC-URSI Radio Science Meeting (Joint with AP-S Symposium), USNC-URSI 2017, Institute of Electrical and Electronics Engineers Inc.; 2017, p. 89–90. https://doi.org/10.1109/USNC-URSI.2017.8074911.
- [5] Zhang H, Zhang L, Gao Q, Xiao Y, Hong H, Zhu X. Body Movement Cancellation Based on Hybrid Radar-Webcam Sensing System. IEEE MTT-S 2019 International Microwave Biomedical Conference, IMBioC 2019 - Proceedings, Institute of Electrical and Electronics Engineers Inc.; 2019. https://doi.org/10.1109/IMBIOC.2019.8777873.
- [6] JalaliBidgoli F, Moghadami S, Ardalan S. A Compact Portable Microwave Life-Detection Device for Finding Survivors. IEEE Embedded Systems Letters 2016;8:10–3. https://doi.org/10.1109/LES.2015.2489209.
- [7] Wu CW, Huang ZY. Using the phase change of a reflected microwave to detect a human subject behind a barrier. IEEE Transactions on Biomedical Engineering 2008;55:267–72. https://doi.org/10.1109/TBME.2007.910680.
- [8] Liu S, Song Y, Zhang M, Zhao J, Yang S, Hou K. An Identity Authentication Method Combining Liveness Detection and Face Recognition. Sensors 2019, Vol 19, Page 4733 2019;19:4733. https://doi.org/10.3390/S19214733.
- [9] Shi M, Wang H, Sun J, Liu C, Huang Z, Zhang B. Face liveness detection benchmark based on stereo matching. ACM International Conference Proceeding Series 2019. https://doi.org/10.1145/3349801.3349811.
- [10] Hassan MA, Mustafa MN, Wahba A. Automatic liveness detection for facial images. Proceedings of ICCES 2017 12th International Conference on Computer Engineering and Systems 2018;2018-January:215–20. https://doi.org/10.1109/ICCES.2017.8275306.
- [11] Sun L, Pan G, Wu Z, Lao S. Blinking-Based Live Face Detection Using Conditional Random Fields. Lecture Notes in Computer Science (Including Subseries Lecture Notes in Artificial Intelligence and Lecture Notes in Bioinformatics) 2007;4642 LNCS:252–60. https://doi.org/10.1007/978-3-540-74549-5_27.
- [12] Menotti D, Chiachia G, Pinto A, Schwartz WR, Pedrini H, Falcão AX, et al. Deep Representations for Iris, Face, and Fingerprint Spoofing Detection. IEEE Transactions on Information Forensics and Security 2015;10:864–79. https://doi.org/10.1109/TIFS.2015.2398817.
- [13] Jung E, Hong K. Biometric verification based on facial profile images for mobile security. Journal of Systems and Information Technology 2015;17:91–100. https://doi.org/10.1108/JSIT-03-2014-0020/FULL/PDF.
- [14] GuangZhu X, PanLong Y, BangJun L, YaoBin Z, JiQuan Y. Eye Region Activity State based Face Liveness Detection System. International Journal of Security and Its Applications 2016;10:361–74. https://doi.org/10.14257/ijsia.2016.10.1.33.
- [15] Lee TW, Ju GH, Liu HS, Wu YS. Liveness detection using frequency entropy of image sequences. ICASSP, IEEE International Conference on Acoustics, Speech and Signal Processing Proceedings 2013:2367–70. https://doi.org/10.1109/ICASSP.2013.6638078.
- [16] Park E, Kim W, Li Q, Kim H, Kim J. Fingerprint liveness detection using CNN features of random sample patches: Liveness detection using CNN features. Lecture Notes in Informatics (LNI),

- Proceedings Series of the Gesellschaft Fur Informatik (GI) 2016;P-260. https://doi.org/10.1109/BIOSIG.2016.7736923.
- [17] Ghiani L, Yambay DA, Mura V, Marcialis GL, Roli F, Schuckers SA. Review of the Fingerprint Liveness Detection (LivDet) competition series: 2009 to 2015. Image and Vision Computing 2017;58:110–28. https://doi.org/10.1016/J.IMAVIS.2016.07.002.
- [18] Lavrentyeva G, Kudashev O, Melnikov A, de Marsico M, Matveev Y. Interactive Photo Liveness for Presentation Attacks Detection. Lecture Notes in Computer Science (Including Subseries Lecture Notes in Artificial Intelligence and Lecture Notes in Bioinformatics) 2018;10882 LNCS:252–8. https://doi.org/10.1007/978-3-319-93000-8_29.
- [19] Dong J, Tian C, Xu Y. Face liveness detection using color gradient features. 2017 International Conference on Security, Pattern Analysis, and Cybernetics, SPAC 2017 2018;2018-January:377–82. https://doi.org/10.1109/SPAC.2017.8304308.
- [20] Al-Naji A, Perera AG, Mohammed SL, Chahl J. Life Signs Detector Using a Drone in Disaster Zones. Remote Sensing 2019, Vol 11, Page 2441 2019;11:2441. https://doi.org/10.3390/RS11202441.
- [21] Maiman TH. Stimulated Optical Radiation in Ruby. Nature 1960 187:4736 1960;187:493–4. https://doi.org/10.1038/187493a0.
- [22] Nasim H, Jamil Y. Diode lasers: From laboratory to industry. Optics and Laser Technology 2014;56:211–22. https://doi.org/10.1016/j.optlastec.2013.08.012.
- [23] Schnabel R. Squeezed states of light and their applications in laser interferometers. Physics Reports 2017;684:1–51. https://doi.org/10.1016/j.physrep.2017.04.001.
- [24] Yu TY. Laser-based sensing for assessing and monitoring civil infrastructures. Sensor Technologies for Civil Infrastructures, vol. 1, Elsevier Inc.; 2014, p. 327–56. https://doi.org/10.1533/9780857099136.327.
- [25] Lutzmann P, Göhler B, van Putten F, Hill CA. Laser vibration sensing: overview and applications. In: Kamerman GW, Steinvall O, Bishop GJ, Gonglewski JD, Lewis KL, Hollins RC, et al., editors. Electro-Optical Remote Sensing, Photonic Technologies, and Applications V, 2011, p. 818602. https://doi.org/10.1117/12.903671.
- [26] Lutzmann P, Göhler B, Hill CA, Putten F van. Laser vibration sensing at Fraunhofer IOSB: review and applications. Optical Engineering 2016;56:031215. https://doi.org/10.1117/1.OE.56.3.031215.
- [27] Zalevsky Z, Beiderman Y, Margalit I, Gingold S, Teicher M, Mico V, et al. Simultaneous remote extraction of multiple speech sources and heart beats from secondary speckles pattern. Optics Express 2009;17:21566–80. https://doi.org/10.1364/OE.17.021566.
- [28] Yazdanfar S, Kulkarni MD, Izatt JA. High resolution imaging of in vivo cardiac dynamics using color Doppler optical coherence tomography. Optics Express 1997;1:424. https://doi.org/10.1364/OE.1.000424.
- [29] Cikajlo I, Šprager S, Erjavec T, Zazula D. Cardiac arrhythmia alarm from optical interferometric signals during resting or sleeping for early intervention. Biocybernetics and Biomedical Engineering 2016;36:267–75. https://doi.org/10.1016/j.bbe.2015.12.006.
- [30] Šprager S, Zazula D. Detection of heartbeat and respiration from optical interferometric signal by using wavelet transform. Computer Methods and Programs in Biomedicine 2013;111:41–51. https://doi.org/10.1016/j.cmpb.2013.03.003.
- [31] Leader in Optical Measurement Equipment Polytec n.d. https://www.polytec.com/eu/ (accessed February 6, 2020).
- [32] Scalise L, Morbiducci U, Melis M De. A laser Doppler approach to cardiac motion monitoring: effects of surface and measurement position. SPIE Proceedings, vol. 6345, 2006, p. 63450D-63450D 11. https://doi.org/10.1117/12.693151.
- [33] Scalise L, Morbiducci U. Non-contact cardiac monitoring from carotid artery using optical vibrocardiography. Medical Engineering & Physics 2008;30:490–7. https://doi.org/10.1016/j.medengphy.2007.05.008.
- [34] De Melis M, Morbiducci U, Scalise L. Identification of cardiac events by Optical Vibrocardiograpy: Comparison with Phonocardiography. Annual International Conference of the IEEE Engineering in Medicine and Biology Proceedings, 2007. https://doi.org/10.1109/IEMBS.2007.4352949.
- [35] Yufu Qu, Tao Wang, Zhigang Zhu. Remote audio/video acquisition for human signature detection. 2009 IEEE Computer Society Conference on Computer Vision and Pattern Recognition Workshops, IEEE; 2009, p. 66–71. https://doi.org/10.1109/CVPRW.2009.5204294.
- [36] Marchionni P, Scalise L, Antonioli L, nobile S, Carnielli VP. Non-contact procedure to measure heart and lung activities in preterm pediatric patients with skin disorders. In: Longo L, editor. Laser Florence 2017: Advances in Laser Medicine, vol. 10582, SPIE; 2018, p. 20. https://doi.org/10.1117/12.2316345.
- [37] Takano C, Ohta Y. Heart rate measurement based on a time-lapse image. Medical Engineering and Physics 2007;29:853–7. https://doi.org/10.1016/j.medengphy.2006.09.006.

- [38] Ozana N, Margalith I, Beiderman Y, Kunin M, Campino GA, Gerasi R, et al. Demonstration of a Remote Optical Measurement Configuration That Correlates with Breathing, Heart Rate, Pulse Pressure, Blood Coagulation, and Blood Oxygenation. Proceedings of the IEEE 2015;103:248–62. https://doi.org/10.1109/JPROC.2014.2385793.
- [39] Olgun N, Türkoğlu İ. Lazer İşaretleri ile Otomatik Hedef Tanıma. Sakarya University Journal of Computer and Information Sciences 2018;1:1–10.
- [40] Olgun N, Türkoğlu İ. Defining materials using laser signals from long distance via deep learning. Ain Shams Engineering Journal 2022;13:101603. https://doi.org/10.1016/J.ASEJ.2021.10.001.
- [41] Gülsoy M. Lazerlerin Tıptaki Uygulamaları n.d.
- [42] LeCun Y, Bengio Y, Hinton G. Deep learning. Nature 2015;521:436–44. https://doi.org/10.1038/nature14539.
- [43] Hinton GE, Salakhutdinov RR. Reducing the dimensionality of data with neural networks. Science 2006. https://doi.org/10.1126/science.1127647.
- [44] Cireşan DC, Meier U, Gambardella LM, Schmidhuber J. Handwritten Digit Recognition with a Committee of Deep Neural Nets on GPUs. ArXiv Preprint ArXiv:11034487 2011.
- [45] Huang Z, Dong M, Mao Q, Zhan Y. Speech emotion recognition using CNN. MM 2014 Proceedings of the 2014 ACM Conference on Multimedia, 2014, p. 801–4. https://doi.org/10.1145/2647868.2654984.
- [46] Palaz D, Magimai-Doss M, Collobert R. Analysis of CNN-based speech recognition system using raw speech as input. Proceedings of the Annual Conference of the International Speech Communication Association, INTERSPEECH, vol. 2015- Janua, 2015, p. 11–5.
- [47] Zhang JS, Xiao XC. Predicting chaotic time series using recurrent neural network. Chinese Physics Letters 2000;17:88–90. https://doi.org/10.1088/0256-307X/17/2/004.
- [48] Kalchbrenner N, Blunsom P. Recurrent continuous translation models. EMNLP 2013 2013 Conference on Empirical Methods in Natural Language Processing, Proceedings of the Conference, Association for Computational Linguistics; 2013, p. 1700–9.
- [49] Cho K, Van Merriënboer B, Gulcehre C, Bahdanau D, Bougares F, Schwenk H, et al. Learning phrase representations using RNN encoder-decoder for statistical machine translation. EMNLP 2014 2014 Conference on Empirical Methods in Natural Language Processing, Proceedings of the Conference, 2014, p. 1724–34. https://doi.org/10.3115/v1/d14-1179.
- [50] Morioka T, Iwata T, Hori T, Kobayashi T. Multiscale recurrent neural network based language model. Proceedings of the Annual Conference of the International Speech Communication Association, INTERSPEECH, vol. 2015- Janua, 2015, p. 2366–70.
- [51] Greff K, Srivastava RK, Koutnik J, Steunebrink BR, Schmidhuber J. LSTM: A Search Space Odyssey. IEEE Transactions on Neural Networks and Learning Systems 2017;28:2222–32. https://doi.org/10.1109/TNNLS.2016.2582924.
- [52] Fushiki T. Estimation of prediction error by using K-fold cross-validation. Statistics and Computing 2011;21:137–46. https://doi.org/10.1007/s11222-009-9153-8.
- [53] Kiran R, Kumar P, Bhasker B. Oslcfit (organic simultaneous LSTM and CNN Fit): A novel deep learning based solution for sentiment polarity classification of reviews. Expert Systems with Applications 2020;157:113488. https://doi.org/10.1016/j.eswa.2020.113488.